CANCER BIOLOGY & THERAPY
2021, VOL. 22, NOS. 7–9, 440–454
https://doi.org/10.1080/15384047.2021.1959792

Taylor & Francis
Taylor & Francis Group

RESEARCH PAPER

circ_C20orf11 enhances DDP resistance by inhibiting miR-527/YWHAZ through the promotion of extracellular vesicle-mediated macrophage M2 polarization in ovarian cancer

Jun Yin[a#], Hai-Yan Huang[b#], Ying Long[c], Yan Ma[d], Maerkeya Kamalibaike[d], Reyanguli Dawuti[d], and Li Li[d]

[a]Department of Pharmacy, Affiliated Tumor Hospital of Xinjiang Medical University, Urumqi, P.R. China; [b]Department of Medical Image Center, The Frist Affiliated Hospital of Xinjiang Medical University, Urumqi, P.R. China; [c]Translational Medicine Center, Hunan Cancer Hospital, Changsha, Hunan Province, P.R. China; [d]Department of Gynecology, Affiliated Tumor Hospital of Xinjiang Medical University, Urumqi, P.R. China

ABSTRACT

Ovarian cancer is a fatal gynecologic tumor, and conventional treatment is mainly limited by chemoresistance. The mechanism contributing to chemoresistance in ovarian cancer has yet to be established. This study aimed to investigate the specific role of circ_C20orf11 in regulating chemoresistance to cisplatin (DDP)in ovarian cancer. We first established two DDP-resistant ovarian cancer cell lines. Then, we identified the effect of circ_C20orf11 on specific cellular characteristics (proliferation, apoptosis, DDP resistance) via a series of experiments. The binding sites between circ_C20orf11 and miR-527 and between miR-527 and YWHAZ were predicted using a bioinformatics tool and confirmed with a dual-luciferase reporter assay. Furthermore, extracellular vesicles (EVs) derived from DDP-resistant cell lines were identified, and the effect of EVs on macrophage polarization was examined. circ_C20orf11 was upregulated in ovarian cancer. Increased circ_C20orf11 expression enhanced DDP resistance and cell proliferation and reduced cell apoptosis in DDP-resistant cell lines after DDP treatment by sponging miR-527 and promoting YWHAZ expression. In addition, we found that DDP-resistant cell-derived EVs can induce macrophage M2 polarization, whereas silencing of circ_C20orf11 inhibited EV-induced macrophage M2 polarization. Consistent with these results, silencing of circ_C20orf11 enhanced sensitivity to DDP in vivo. Importantly, we proved that circ_C20orf11 expression was upregulated in EVs extracted from the serum of DDP-resistant patients. Our study demonstrated that silencing circ_C20orf11 sensitizes ovarian cancer to DDP by promoting miR-527/YWHAZ signaling and EV-mediated macrophage M2 polarization.

ARTICLE HISTORY
Received 21 December 2020
Revised 8 July 2021
Accepted 12 July 2021

KEYWORDS
circ_C20orf11; miR-527; YWHAZ; EVs; ovarian cancer cells; cisplatin; M2 macrophage polarization

Introduction

Ovarian cancer is responsible for the high mortality associated with gynecological malignancies, which cause approximately 125,000 deaths annually on a global scale.[1] Currently, surgery followed by cisplatin (DDP)-based chemotherapy is the standard treatment for ovarian cancer.[1–3] However, most patients relapse within one to two years, and chemoresistance to anticancer drugs is one of the most important factors contributing to the poor survival rates of ovarian cancer patients.[4,5] Hence, understanding the mechanisms underlying chemoresistance in ovarian cancer is crucial for enhancing sensitivity to DDP-based chemotherapy or developing new targeted drugs.

As the most abundant cells in the tumor microenvironment, tumor-associated macrophages may promote tumor progression, metastasis, and chemoresistance.[6–8] Nevertheless, it is not entirely clear why macrophages polarize into tumor-associated macrophages in the tumor microenvironment.[9] Extracellular vesicles (EVs), which are secreted by cells into the extracellular space, include exosomes, apoptotic bodies, and microvesicles. Recent studies have indicated that EVs can regulate macrophage polarization[9–11] and mediate communication in the tumor microenvironment by transferring genetic information, including functional messenger RNAs (mRNAs) and microRNAs (miRNAs), to target cells or organs.[12–14] Liang et al. reported that EVs derived from ovarian cancer patients may be highly involved in ovarian cancer progression or chemoresistance.[13] However, the relationships among EVs, RNAs, and tumor-associated macrophages in ovarian cancer chemoresistance require further establishment.

As a member of the noncoding RNA (ncRNA) family, circular RNAs (circRNAs) have been identified to play a crucial role in many pathological processes, such as cancer processes.[15–18] circRNAs can mediate the biological activities of miRNAs.[15–18] Previous reports identified that circRNAs were abnormally expressed during ovarian cancer development.[15–18] We observed that circ_C20orf11 expression in ovarian cancer was abnormally upregulated, and yet, the specific role of circ_C20orf11 in ovarian cancer and whether it is associated with chemoresistance in ovarian cancer remain to be elucidated.

In this study, we investigated circ_C20orf11 expression and its biological significance in DDP resistance in ovarian cancer

CONTACT Li Li zzxcdd789@163.com Department of Gynecology, Affiliated Tumor Hospital of Xinjiang Medical University, No.789, Suzhou Street, Xinshi District, Urumqi, 830011, Xinjiang Uygur Autonomous Region, P.R. China
[#]These are co-first authors

cells. Our results indicated that circ_C20orf11 promotes EV-mediated M2 macrophage polarization by inhibiting miR-527/tyrosine 3-monooxygenase/tryptophan 5-monooxygenase activation protein zeta (YWHAZ) signaling, in turn promoting DDP resistance in vitro and in vivo. This study provides evidence that circ_C20orf11 may contribute to new therapeutic strategies against ovarian cancer.

Results

circ_C20orf11 enhances DDP resistance in ovarian cancer cells

According to previous studies, abnormal circRNA expression is associated with tumor development, including ovarian cancer development.[1,15,19] A recently published paper revealed that abnormal expression of circ_C20orf11 is related to the development of ovarian cancer.[19] To determine whether circ_C20orf11 is involved in DDP resistance in ovarian cancer cells, the circ_C20orf11 gene expression level was first assessed in ovarian epithelial cells and ovarian cancer cell lines. The expression of circ_C20orf11 was increased in ovarian cancer cell lines, with higher levels observed in A2780 and SKOV3 cells, which were therefore selected for the following experiments (Figure 1(a)). We next established DDP-resistant SKOV3 and A2780 (SKOV3/DDP, A2780/DDP) cell lines. circ_C20orf11 expression was significantly upregulated in the SKOV3/DDP and A2780/DDP cells compared to the parental cells (Figure 1(b)). The effects of serial concentrations of DDP on SKOV3 cell, SKOV3/DDP cell, A2780 cell, and A2780/DDP cell viability were assessed using MTT assays. The results indicated that cell viability was reduced with increasing DDP concentration in all cell types (Figure 1(c)). SKOV3/DDP and A2780/DDP cells showed higher cell viability than parental cells upon DDP treatment. The IC50 value of DDP was significantly increased in SKOV3/DDP and A2780/DDP cells (Figure 1(d)).

To establish the specific role of circ_C20orf11 in the DDP-resistance mechanism of ovarian cancer cells, SKOV3/DDP and A2780/DDP cells were transfected with siRNA against circ_C20orf11. qPCR results confirmed that circ_C20orf11 was successfully knocked down in SKOV3/DDP and A2780/DDP cells (Figure 1(e)). circ_C20orf11-silenced SKOV3/DDP and A2780/DDP cells were treated with serial concentrations of DDP, and cell viability was assessed via MTT assays (Figure 1(f)). Silencing of circ_C20orf11 reduced the viability of SKOV3/DDP and A2780/DDP cells compared to their negative controls upon DDP treatment. Knockdown of circ_C20orf11 also decreased the IC_{50} value of DDP in both SKOV3/DDP and A2780/DDP cells (Figure 1(g)). Thus, circ_C20orf11 enhances DDP resistance in ovarian cancer cells.

circ_C20orf11 regulates DDP-resistant ovarian cancer cell proliferation and apoptosis

Knockdown of circ_C20orf11 in SKOV3/DDP cells, A2780/DDP cells, SKOV3 cells and A2780 cells reduced the colony number upon DDP treatment in comparison to the correlated siRNA negative controls, indicating that depletion of circ_C20orf11 suppressed both DDP-resistant and DDP-sensitive ovarian cell proliferation (Figure 2(a)). Consistently, silencing of circ_C20orf11 in SKOV3/DDP cells, A2780/DDP cells, SKOV3 cells, and A2780 cells further increased the apoptotic rate upon DDP treatment relative to the correlated siRNA negative controls (Figure 2(b-d)). In summary, our data suggest that circ_C20orf11 enhances both DDP-resistant and DDP-sensitive ovarian cancer cell proliferation and inhibits cell apoptosis.

circ_C20orf11 directly binds to miR-527, and miR-527 directly targets YWHAZ

Numerous studies have indicated that circRNAs regulate gene expression by acting as competing endogenous RNAs.[15–18] Our bioinformatics analyses indicated that circ_C20orf11 may potentially target miR-527 (Figure 3(a)). miR-527 gene expression was significantly downregulated in both SKOV3/DDP cells and A2780/DDP cells compared to that in their parental cells (Figure 3(b)). In contrast, knockdown of circ_C20orf11 increased miR-527 expression in SKOV3/DDP cells and A2780/DDP cells, indicating that miR-527 may play a role in circ_C20orf11 regulation of DDP resistance in ovarian cancer cells (Figure 3(c)). SKOV3/DDP cells and A2780/DDP cells were transfected with miR-527 mimic or miR-527 inhibitor, and the success of the transfection was confirmed by qPCR data (Figure 3(d)). A significant decrease in the relative luciferase activity of wild-type circ_C20orf11 (C20orf11-WT) was detected when cells were cotransfected with the miR-527 mimic but not when the vector contained a mutation in the miR-527 binding site sequence (C20orf11-MUT; Figure 3(e)). In addition, the relative luciferase activity of wild-type circ_C20orf11 was significantly increased when cells were cotransfected with the miR-527 inhibitor but not when cells were cotransfected with a vector encoding a mutation in the miR-527 binding site sequence.

YWHAZ expression was significantly upregulated in both SKOV3/DDP cells and A2780/DDP cells compared to their parental cells (Figure 3(g)). However, silencing of circ_C20orf11 led to downregulation of YWHAZ in SKOV3/DDP cells and A2780/DDP cells (Figure 3(h)). Bioinformatics analyses revealed that YWHAZ potentially targeted the 3′-UTR of miR-527 (Figure 3(f)). Following transfection of SKOV3/DDP and A2780/DDP cells with miR-527 mimic, YWHAZ was significantly decreased (Figure 3(i)). In contrast, transfection of SKOV3/DDP and A2780/DDP cells with miR-527 inhibitor increased YWHAZ expression, suggesting that miR-527 suppresses YWHAZ expression. The interactions between YWHAZ and the 3′UTR of miR-527 were further confirmed by luciferase reporter assay data (Figure 3(j)).

Collectively, these results suggest that miR-527 is a direct target of circ_C20orf11 and that miR-527 directly targets YWHAZ.

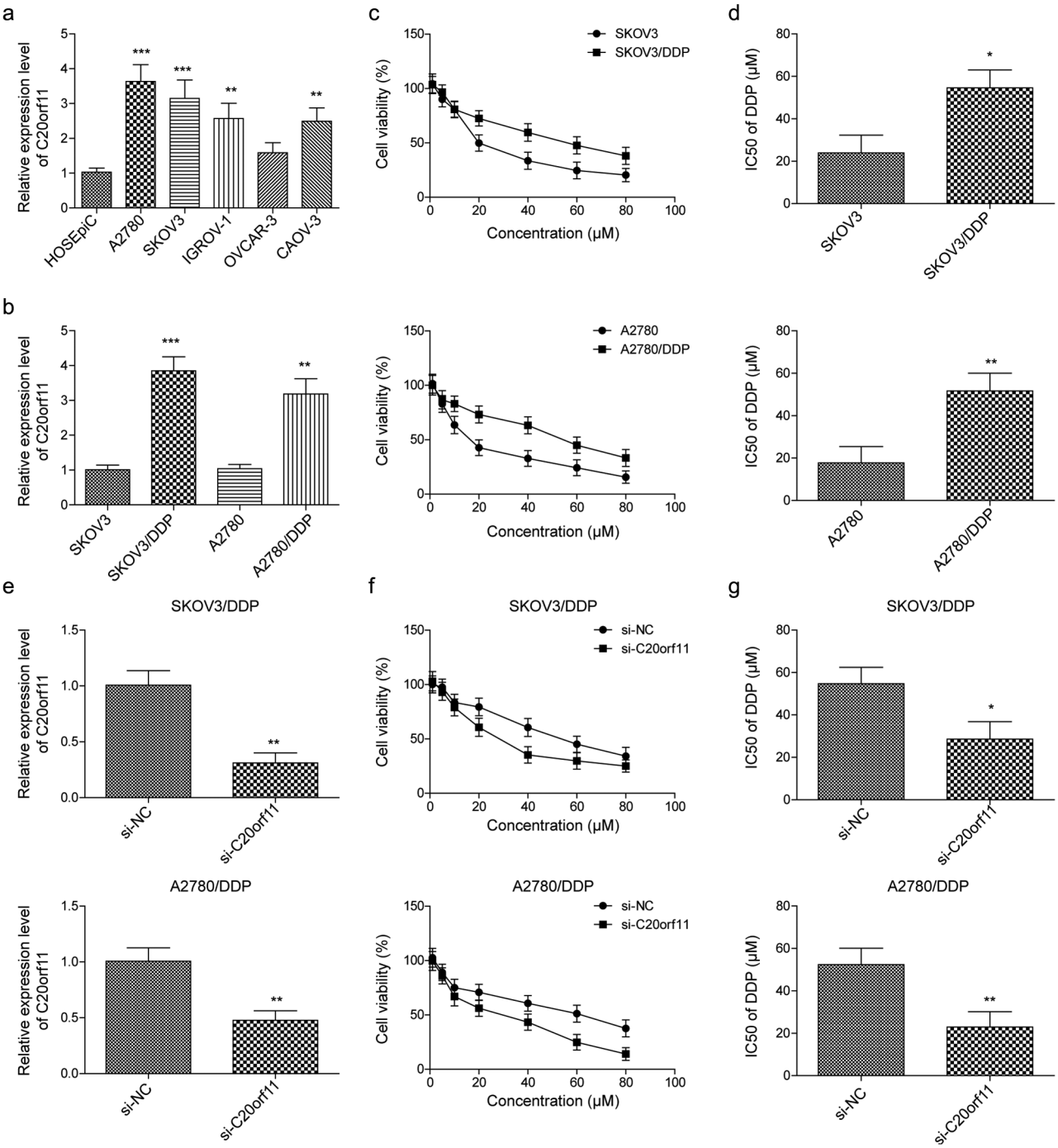

Figure 1. circ_C20orf11 promotes DDP resistance in ovarian cancer cells. (a) Relative gene expression of C20orf11 in ovarian epithelial cells (HOSEpiCs) and ovarian cancer cell lines (A2780, SKOV3, IGR0V-1, OVCAR-3 and CAOV-3). Relative gene expression levels were determined using the comparative Ct method with GAPDH as the reference gene and the formula $2^{-\Delta\Delta Ct}$. (b) Relative gene expression of C20orf11 in DDP-resistant ovarian cancer cell lines and their parental cells in relation to GAPDH and U6 expression. (c) Cell viability in SKOV3/DDP, A2780/DDP and their parental cells upon DDP treatment. (d) The IC50 value of DDP in SKOV3/DDP, A2780/DDP and their parental cells upon DDP treatment. (e) After SKOV3/DDP and A2780/DDP cells were transfected with adenoviral circ_C20orf11 (si-C20orf11) or its vector control (si-NC), the cells were treated with DDP. Relative mRNA expression of C20orf11 in DDP-treated SKOV3/DDP and A2780/DDP cells with or without adenoviral C20orf11 (si-C20orf11+ DDP) or its vector control (si-NC+DDP) transfection. (f) MTT assays were performed to assess cell viability using the same conditions as described in (e). (g) The IC50 value of DDP determined using the same conditions as described in (e). n = 3. *$P < .05$, ** $P < .01$, *** $P < .001$.

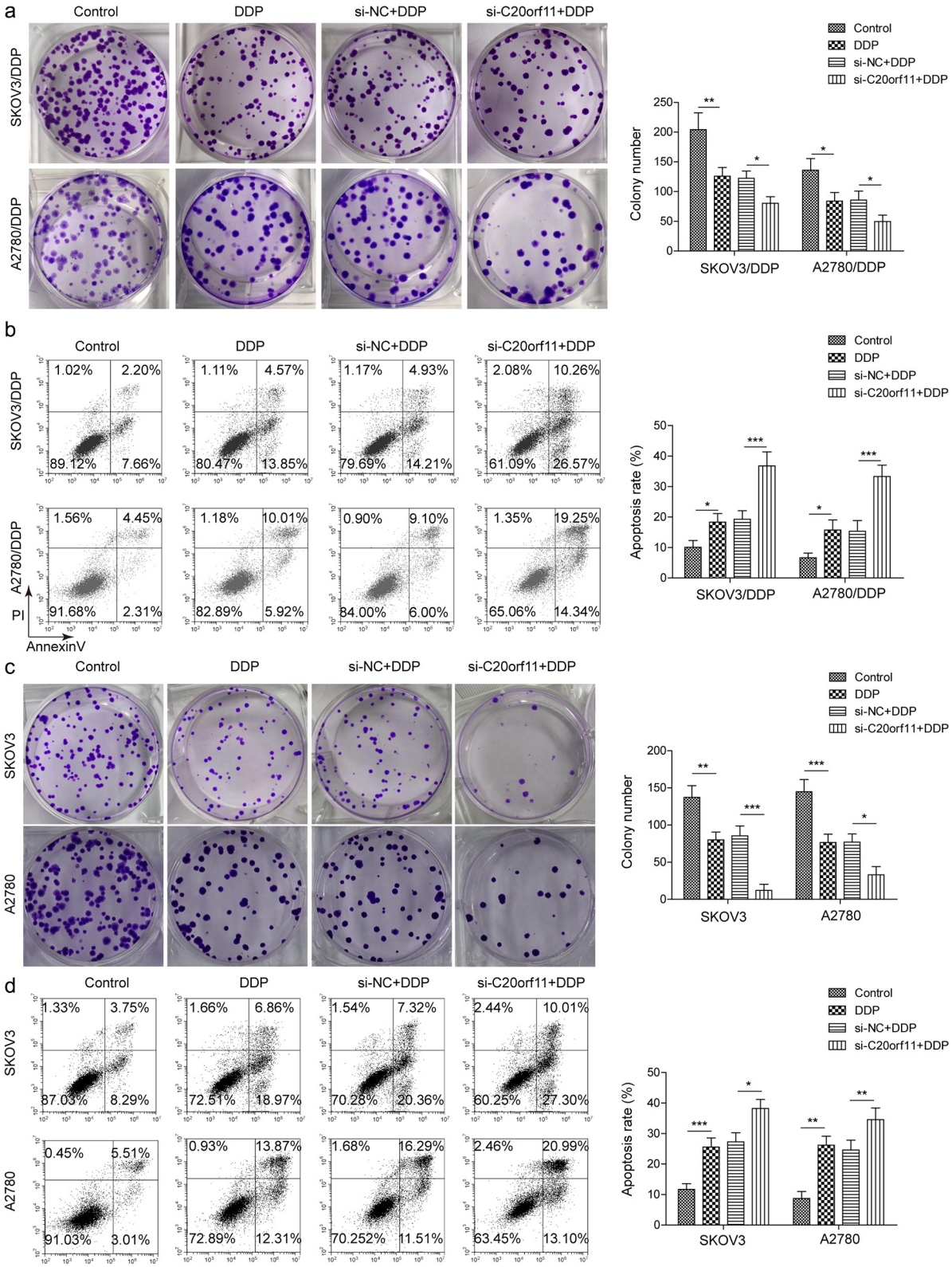

Figure 2. circ_C20orf11 enhances ovarian cancer cell proliferation and suppresses cell apoptosis. (a) After SKOV3/DDP and A2780/DDP cells were transfected with adenoviral circ_C20orf11 (si-C20orf11) or its vector control (si-NC), the cells were treated with DDP. The colony number in DDP-treated SKOV3/DDP and A2780/DDP cells with or without adenoviral C20orf11 or its vector control transfection and the untreated control. (b) The apoptosis rate in DDP-treated SKOV3/DDP and A2780/DDP cells with or without adenoviral C20orf11 (si-C20orf11+ DDP) or its vector control (si-NC+DDP) transfection and the untreated control. (c) After SKOV3 and A2780 cells were transfected with adenoviral circ_C20orf11 or its vector control, the cells were treated with DDP. The relative colony number ratio in DDP-treated SKOV3 and A2780 cells with (si-C20orf1+ DDP) or without adenoviral C20orf11 (DDP) or its vector control transfection (si-NC+DDP) and the untreated control (Control). (d) The apoptosis rate in DDP-treated SKOV3 and A2780 cells with or without adenoviral C20orf11 or its vector control transfection and the untreated control. n = 3. *$P < .05$, ** $P < .01$, *** $P < .001$.

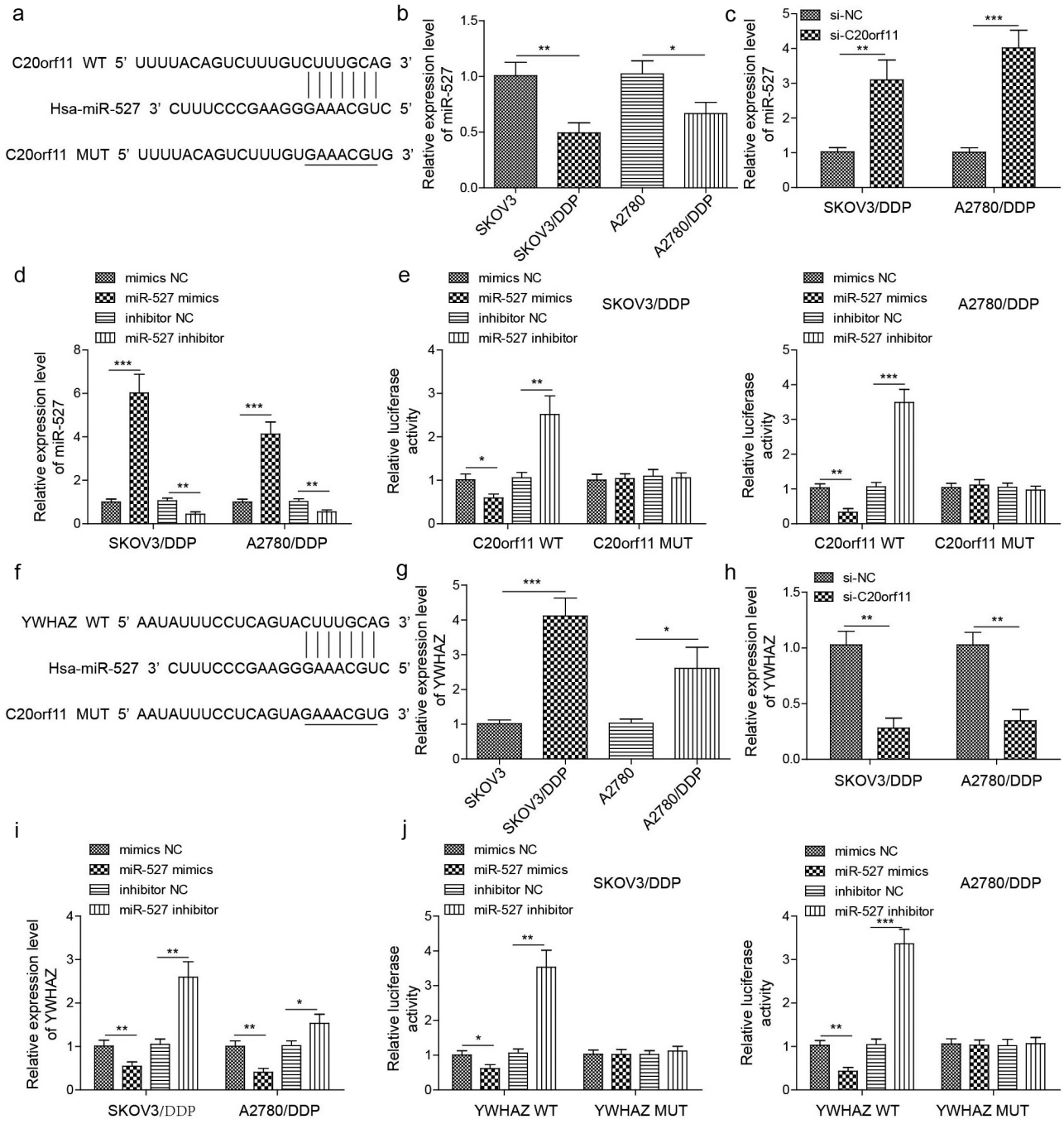

Figure 3. circ-C20orf11 binds to miR-527, and miR-527 targets YWHAZ. (a) Predicted target sites of miR-527 in the 3′-UTR of circ-C20orf11. (b) Relative gene expression of miR-527 in SKOV3/DDP and A2780/DDP cells and their parental cells in relation to GAPDH and U6 expression. (c) SKOV3/DDP or A2780/DDP cells were transfected with adenoviral circ_C20orf11 (si-C20orf11) or its vector control (si-NC). Relative gene expression of miR-527 in SKOV3/DDP or A2780/DDP cells with or without adenoviral C20orf11 or its vector control transfection in relation to GAPDH and U6 expression. (d) SKOV3/DDP or A2780/DDP cells were transfected with miR-527 inhibitor, miR-527 mimic, or a negative control. Relative gene expression of miR-527 in SKOV3/DDP and A2780/DDP cells with or without miR-527 mimic or miR-527 inhibitor or their related negative control transfection as well as untreated controls. (e) SKOV3/DDP or A2780/DDP cells were cotransfected with miR-527 mimic or a miR-527 inhibitor and circ-C20orf11-WT or circ-C20orf11-MUT. Afterward, luciferase activity was measured. (f) Predicted target sites of YWHAZ in the 3′-UTR of miR-527. (g) Gene expression of YWHAZ in SKOV3/DDP and A2780/DDP cells and their parental cells in relation to GAPDH and U6 expression. (h) SKOV3/DDP and A2780/DDP cells were transfected with adenoviral circ_C20orf11 or its vector control. The gene expression of YWHAZ in SKOV3/DDP and A2780/DDP cells with or without adenoviral C20orf11 or its vector control transfection in relation to GAPDH and U6 expression. (i) SKOV4/DDP and A2780/DDP cells were transfected with miR-527 inhibitor, miR-527 mimic, or a negative control. The gene expression of YWHAZ in relation to GAPDH and U6 expression in SKOV4/DDP and A2780/DDP cells with or without miR-527 mimic or miR-527 inhibitor or their related negative control transfection as well as untreated controls. (j) SKOV4/DDP or A2780/DDP cells were cotransfected with miR-527 mimic or a miR-527 inhibitor and YWHAZ-WT or YWHAZ-MUT. Afterward, luciferase activity was measured. n = 3. *$P < .05$, ** $P < .01$, *** $P < .001$.

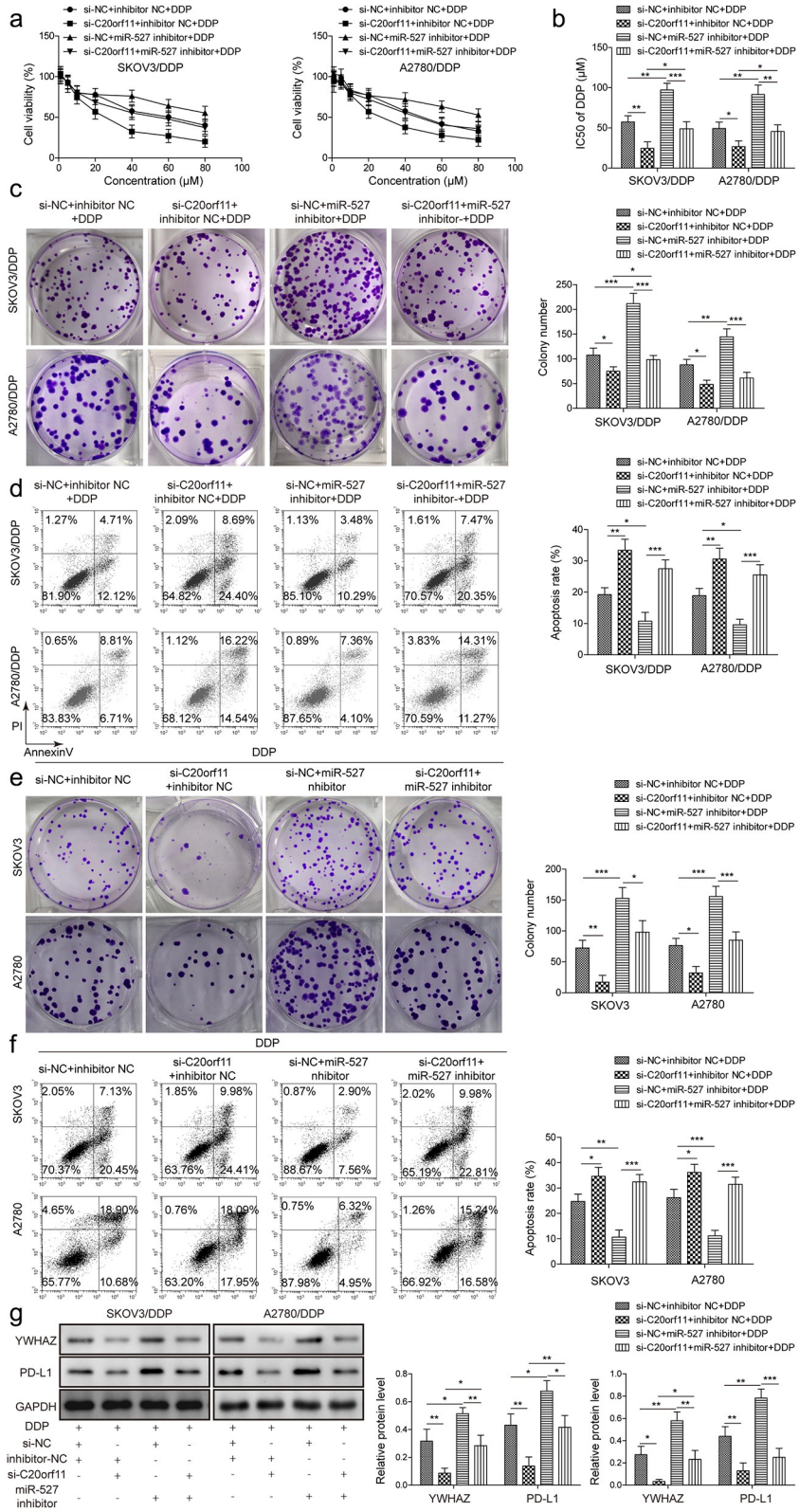

Figure 4. circ_C20orf11 promotes DDP resistance in SKOV3/DDP and A2780/DDP cells by sponging miR-527. (a) After SKOV3/DDP and A2780/DDP cells were transfected with adenoviral circ_C20orf11 or its vector control and miR-527 inhibitor, the cells were treated with DDP. The viability of SKOV3/DDP or A2780/DDP cells with or without adenoviral C20orf11 (si-C20orf11+ inhibitor+NC+DDP) or its vector control (si-NC+inhibitor+NC+DDP) and miR-527 inhibitor transfection. (b) IC50 of DDP using the same conditions as described in (a). (c) Colony formation assays were performed using the same conditions as described in (a). (d) Cell apoptosis assays were performed using the same conditions as described in (a). (e) The relative colony number ratio in DDP-treated SKOV3 and A2780 cells with adenoviral C20orf11/miR-527 inhibitor (si-C20orf1+ DDP + miR-527+ DDP) or with adenoviral C20orf11/miR-527 inhibitor negative control (si-C20orf11+ inhibitor NC+DDP) or vector control transfection/miR-527 inhibitor (si-NC+miR-527 inhibitor+DDP) and the vector control transfection/miR-527 inhibitor negative control (si-NC+inhibitor NC+ DDP). (f) The apoptosis rate in DDP-treated SKOV3 and A2780 cells treated with adenoviral C20orf11/miR-527 inhibitor (si-C20orf1+ DDP + miR-527+ DDP) or with adenoviral C20orf11/miR-527 inhibitor negative control (si-C20orf11+ inhibitor NC+DDP) or vector control transfection/miR-527 inhibitor (si-NC+miR-527 inhibitor+ DDP) and the vector control transfection/miR-527 inhibitor negative control (si-NC+inhibitor NC+ DDP). (g) Western blot analyses using the same conditions as described in (a). n = 3. *$P < .05$, ** $P < .01$, *** $P < .001$.

circ_C20orf11 promotes DDP resistance in SKOV3/DDP and A2780/DDP cells by sponging miR-527

To further evaluate whether miR-527 is involved in circ_C20orf11-mediated DDP resistance in ovarian cancer cells, we treated SKOV3/DDP cells and A2780/DDP cells with a miR-527 inhibitor and si-C20orf11 in combination with DDP treatment. As illustrated in Figure 4(a), miR-527 downregulation reversed the inhibitory effect of circ_C20orf11 knockdown on both SKOV3/DDP cell and A2780/DDP cell viability upon DDP treatment. Furthermore, suppression of miR-527 reversed the inhibitory effect of circ_C20orf11 depletion on reducing the IC50 value for DDP in both SKOV3/DDP cells and A2780/DDP cells upon DDP treatment (Figure 4(b)). Data from colony formation and flow cytometry assays confirmed that depletion of miR-527 rescued silencing of circ_C20orf11-induced inhibition of proliferation and increased apoptosis in SKOV3/DDP cells, A2780/DDP cells, SKOV3 and A2780 cells (Figure 4(c-f)). Moreover, suppression of miR-527 reversed the circ_C20orf11 silencing-induced inhibitory effects on YWHAZ and PD-L1 expression (Figure 4(g)).

Taken together, the data suggest that miR-527 is involved in regulation of YWHAZ/PD-L1 expression. Furthermore, circ_C20orf11 enhances DDP resistance in SKOV3/DDP and A2780/DDP cells by suppressing miR-527.

EVs mediate M2-type macrophage polarization in ovarian cancer

Accumulated evidence has shown that EVs play a crucial role in regulating chemoresistance in ovarian cancer cells.[12,14,20] This regulatory mechanism may occur through macrophage polarization.[14] Thus, we isolated EVs from the supernatant of SKOV3/DDP cells and characterized the EVs using electron microscopy and nanoparticle tracking (Figure 5(a)). The EVs were oval with an average diameter of 100 nm (Figure 5(a,b)). The expression of EV-specific markers (CD9, CD63, and TSG101) was quantified via western blotting (Figure 5(c)). To examine whether the extracted EVs could be taken up by macrophage cells in the tumor microenvironment, EVs from SKOV3/DDP cells were stained with PKH67 dye. As shown by the fluorescence images, the EVs were located in the cytoplasm of macrophage cells (Figure 5(d)). To further delineate whether EVs can influence macrophage polarization, M2-type macrophage cells were treated with EVs derived from SKOV3/DDP cells and A2780/DDP cells. EV-treated cells had significantly higher interleukin-10 (IL-10) expression than untreated cells (Figure 5(e)). However, knockdown of circ_C20orf11 reversed the EV-induced increase in IL-10 expression in macrophages. Furthermore, cells treated with EVs had significantly lower expression of IL-6, tumor necrosis factor-alpha (TNF-α), and inducible nitric oxide synthase (iNOS), which have been suggested to be M1 macrophage markers (Figure 5(f,g)). Silencing of circ_C20orf11 reversed the EV-induced inhibitory effect on TNF-α, IL-6 and iNOS expression. Moreover, EV treatment of SKOV3/DDP cells and A2780/DDP cells significantly promoted CD206, IL-10 and Arg-1 expression, which are considered M2 macrophage markers (Figure 5(h)). Nevertheless, depletion of circ_C20orf11 reversed the EV-induced stimulation effects on CD206, IL-10 and Arg-1 expression.

Thus, EVs isolated from DDP-resistant ovarian cells can induce macrophage M2 polarization, whereas silencing of circ_C20orf11 inhibits EV-induced macrophage M2 polarization.

Silencing of circ_C20orf11 enhances DDP sensitivity in vivo

To further elucidate the effect of circ_C20orf11 on DDP sensitivity in vivo, mouse models were established by subcutaneous injection of SKOV3/DDP or A2780/DDP cells and treatment with PBS or DDP (n = 5 per group). Notably, depletion of circ_C20orf11 significantly reduced tumor volume and tumor weight in comparison to the negative control group upon DDP treatment (Figure 6(a-c)). These findings further highlight the role of circ_C20orf11 in chemoresistance to DDP in vivo. qPCR results showed that knockdown of circ_C20orf11 significantly upregulated miR-527 but downregulated YWHAZ compared to levels in the si-NC group (Figure 6(d)). The expression levels of IL-6, TNF-α, and iNOS were significantly upregulated in the circ_C20orf11-depleted group upon DDP treatment (Figure 6(e)). Conversely, the marker proteins CD206, IL-10 and Arg-1 were downregulated in the circ_C20orf11-depleted group upon DDP treatment (Figure 6(f)). Western blotting results verified that silencing of circ_C20orf11 reduced the expression of YWHAZ and programmed death-ligand 1 (PD-L1) (Figure 6(g)).

Overall, knockdown of circ_C20orf11 increases DDP sensitivity in mouse models.

Serum EV-circ_C20orf11 levels are upregulated in ovarian patients

Finally, we compared the circ_C20orf11 level in ovarian cancer samples from DDP-sensitive ovarian cancer patients and DDP-resistant ovarian cancer patients. The expression of circ_C20orf11 was significantly increased but miR-527 expression was decreased in the DDP-resistant group compared to the DDP-sensitive group (Figure 7(a,b)). The flow cytometry results indicated a significantly enhanced number of CD206-positive cells in the DDP-resistant group relative to the number in the DDP-sensitive group and healthy group (Figure 7(c)). qPCR results further indicated that CD206 gene expression was significantly upregulated in the DDP-resistant group compared to the DDP-sensitive group and the healthy group (Figure 7(d)). To further identify the connections between circ_C20orf11 and miR-527 and between miR-527 and CD206, we performed correlation analyses. The results confirmed that circ_C20orf11 expression was negatively correlated with miR-527 in the tumor tissues of patients with ovarian cancer (Figure 7(e)). Similarly, a significant inverse correlation was observed between miR-527 and CD206 in the tumor tissues of patients with ovarian cancer (Figure 7(f)). To identify whether EVs from ovarian cancer patients contain circ_C20orf11, we extracted EVs from DDP-sensitive and DDP-resistant ovarian cancer patient serum samples. These vesicles were characterized using several methods, including electron microscopy (Figure 7(g)) and nanoparticle tracking (Figure 7(h)). The presence of the EV markers CD63, TSG101

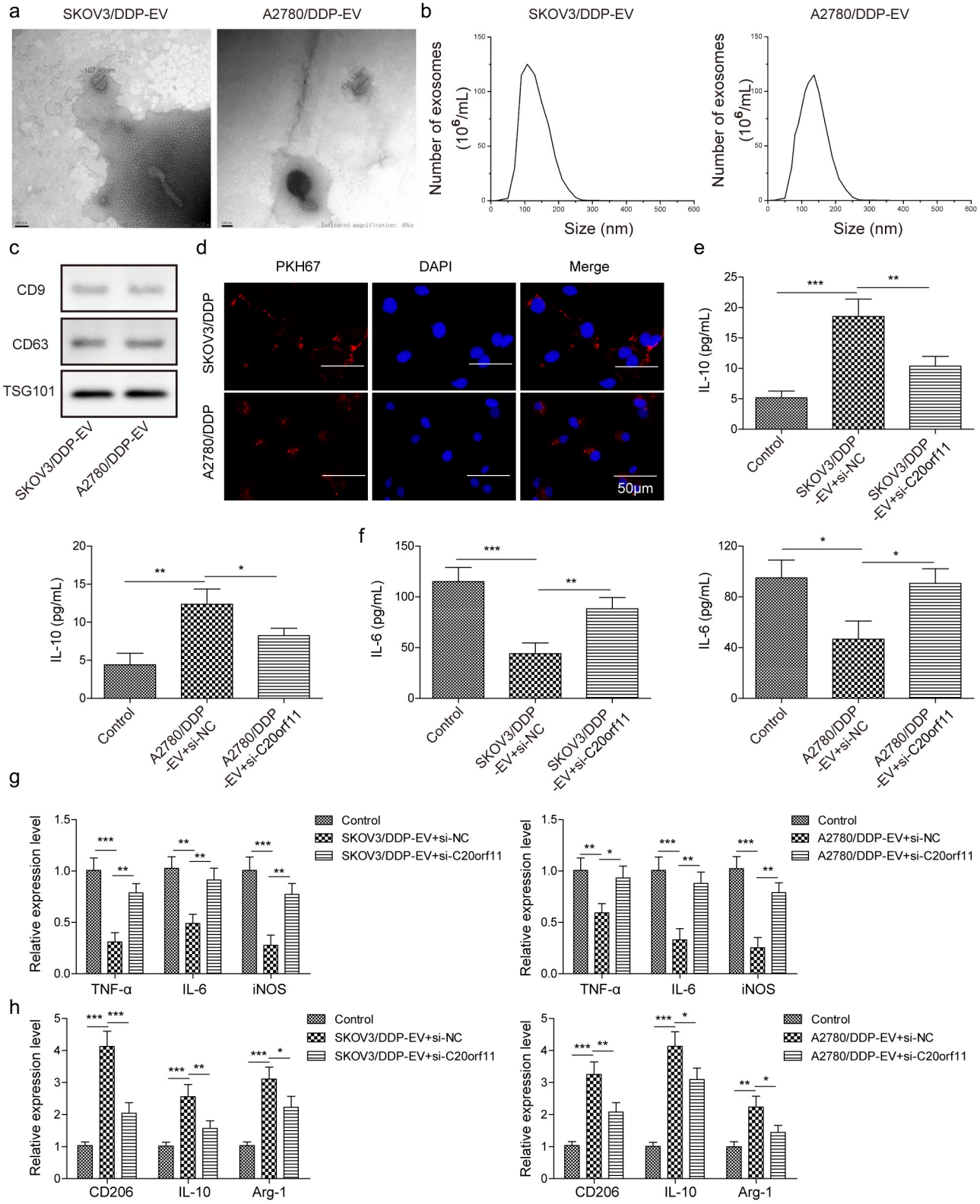

Figure 5. EVs mediate M2-type macrophage polarization in ovarian cancer. (a) EVs were isolated from the supernatant of SKOV3/DDP cells and characterized via electron microscopy and (b) nanoparticle tracking. (C) EV-specific markers (CD9, TSG101 and CD63) were measured via western blotting. (d) EVs were labeled with PKH67 dye and cultured with THP-1 cells. Representative fluorescence images are shown. (e) After SKOV3/DDP and A2780/DDP cells were transfected with adenoviral circ_C20orf11 (si-SKOV3/DDP-Exo+si-C20orf11) or its vector control (si-SKOV3/DDP-Exo+si-NC), the cells were cultured with EVs from SKOV3/DDP cells. IL-10 expression was detected using an ELISA. Untreated THP-1 cells served as the control. (f) An ELISA was performed to detect IL-6 expression. (g) Relative mRNA expression of TNF-α, IL-6 and iNOS. (H) mRNA expression of CD206, IL-10 and Arg-1 in relation to GAPDH and U6 expression. n = 3. *$P < .05$, ** $P < .01$, *** $P < .001$.

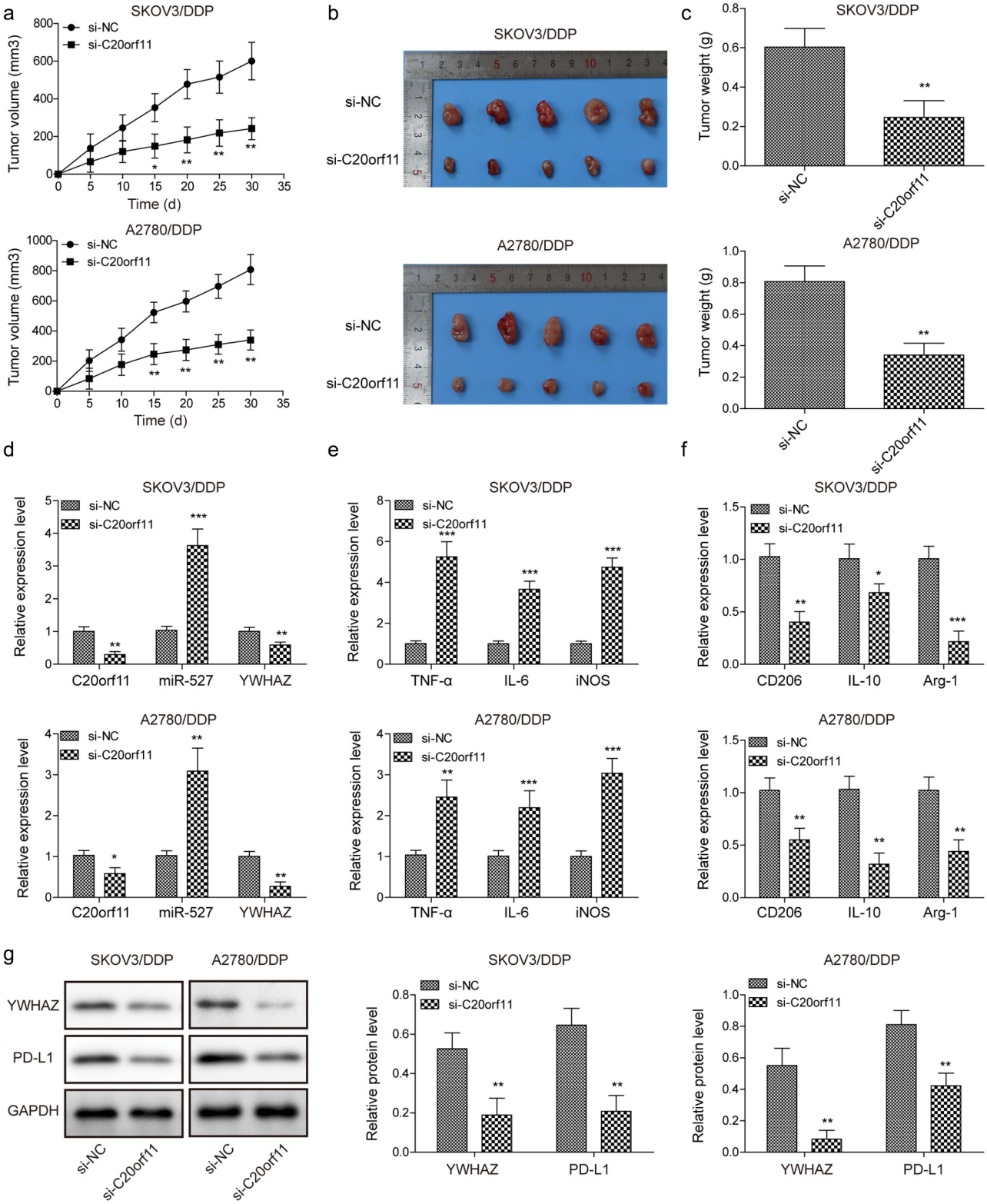

Figure 6. Silencing of circ_C20orf11 enhances sensitivity to DDP in vivo. Xenotransplantation studies were performed with SKOV3 cells. (a) Tumor volume was measured every 5 days for 30 days. (b) Representative images of tumor formation. (c) Tumor weight was measured. (d) qPCR analysis of C20orf11, miR-527 and YWHAZ expression. (e) qPCR results showing CD206, IL-10 and Arg-1 expression. (f) Western blotting detection of YWHAZ PD-L1 is presented. n = 3. *$P < .05$, ** $P < .01$, *** $P < .001$.

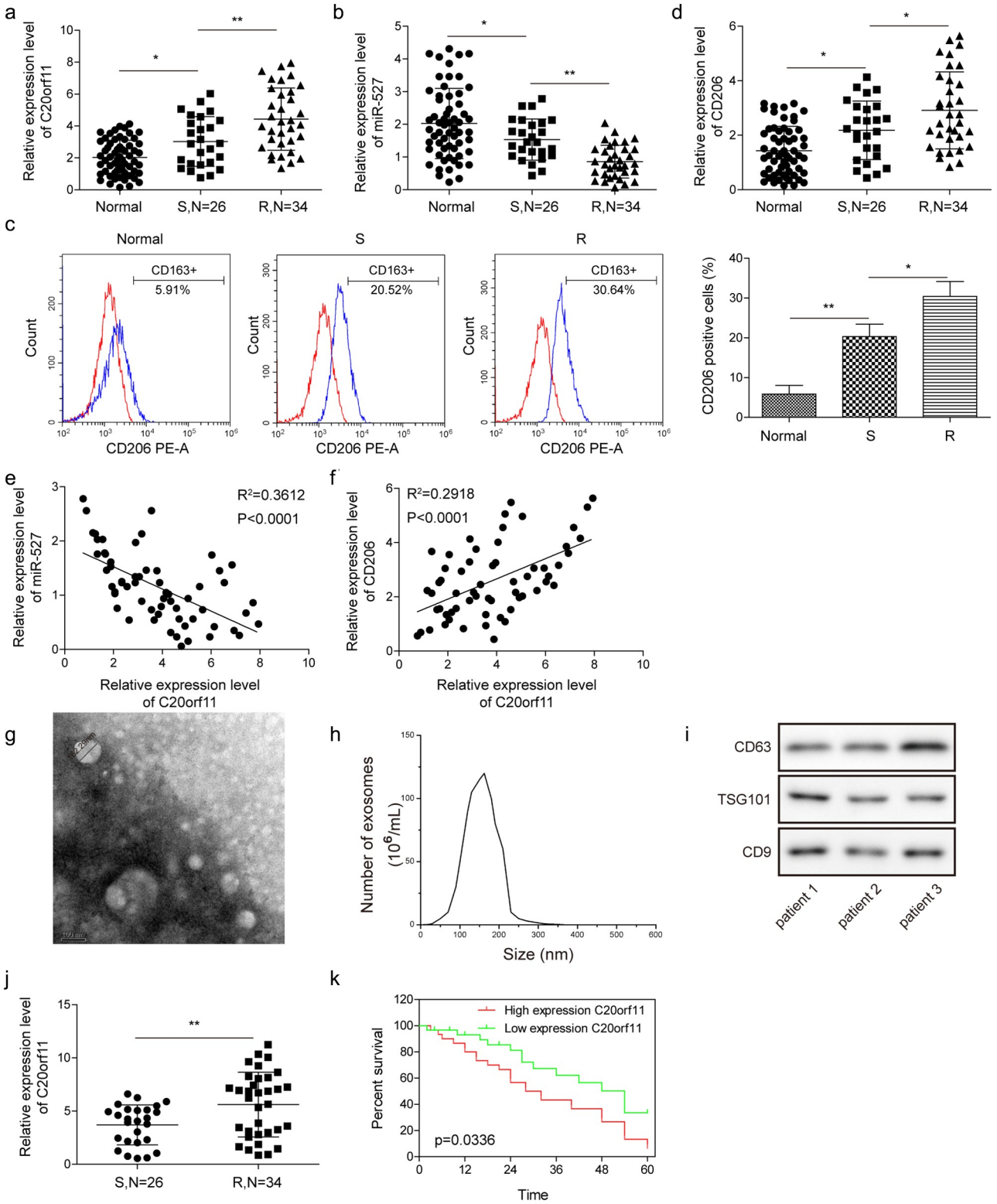

Figure 7. Serum EV-circ_C20orf11 levels are upregulated in ovarian patients. Patients were considered DDP resistant if they showed no significant clinical effect or had progressive disease after receiving one cycle of DDP treatment. The remaining patients were considered DDP sensitive. Real-time qPCR analysis of (a) C20orf11 and (b) miR-527 expression in relation to GAPDH and U6 expression in DDP-sensitive ovarian cancer tissue (S), DDP-resistant ovarian cancer tissue (R), and healthy ovarian tissue (Normal). (c) Flow cytometry detection and quantification of CD206-positive cells in DDP-sensitive ovarian cancer tissue (S), DDP-resistant ovarian cancer tissue (R), and healthy ovarian tissue (Normal). (d) Real-time qPCR analysis of CD206 expression in relation to GAPDH and U6 expression in DDP-sensitive ovarian cancer tissue (S), DDP-resistant ovarian cancer tissue (R), and healthy ovarian tissue (Normal). (e) The expression level of C20orf11 in ovarian cancer tissue was negatively correlated with that of miR-527. (f) The expression level of miR-527 in ovarian cancer tissue was negatively correlated with that of CD206. (g) Representative image of serum EVs detected using an electron microscope. (h) EVs were measured using nanoparticle tracking. (i) EV markers were analyzed via western blotting. (j) The abundance of C20orf11 in serum EVs was assessed using qPCR. (k) Kaplan-Meier survival curves of patients with ovarian cancer with high and low C20orf11 expression. n = 3. *$P < .05$, ** $P < .01$.

Table 1. The association between serum EV-circ_C20orf11 expression and clinicopathological variables in ovarian patients.

	EV-circ_C20orf11 expression		
Clinical parameters	**High (n = 30)**	**Low (n = 30)**	**P value**
Age (years)			
<50	16	12	0.301
≥ 50	14	18	
Histological subtype			
Serous	26	21	0.117
Other	4	9	
FIGO stage			
I–II	2	16	<0.0001
III–IV	28	14	
Histological grade			
G1+ G2	9	17	0.037
G3	21	13	
Lymph node metastasis			
Absent	11	23	0.002
Present	19	7	

and CD9 confirmed the purity of the extracted EVs (Figure 7(i)). qPCR results indicated that circ_C20orf11 expression was detectable in extracted EVs (Figure 7(j)). Furthermore, circ_C20orf11 expression was lower in EVs extracted from the serum of the DDP-sensitive group than in EVs extracted from the serum of the DDP-resistant group. Elevated EV-circ_C20orf11 levels were correlated with advanced FIGO stage, high histological grade and lymph node metastasis (Table 1). Kaplan-Meier survival curves of patients with ovarian cancer are shown in Figure 7(k). The results confirmed that patients with high EV-circ_C20orf11 expression had a relatively poorer survival rate than those with low levels.

These results confirm that the levels EV-circ_C20orf11 in the serum are high in ovarian cancer patients and that an enhanced EV-circ_C20orf11 level is associated with the poor survival rate of ovarian patients.

Discussion

Ovarian cancer a fatal gynecological tumor, and conventional treatment is mostly limited by chemoresistance.[1,2] Understanding the mechanism of chemoresistance can contribute to the treatment of ovarian cancer. This study revealed a critical role of circ_C20orf11 in regulating DDP resistance in ovarian cancer and identified that the regulatory mechanism involved the miR-527/YWHAZ signaling pathway. Furthermore, we demonstrated that EVs from DDP-resistant ovarian cancer cells shuttled circ_C20orf11 and participated in regulating M2 macrophage polarization, thus mediating DDP resistance.

The critical role of noncoding RNA in regulating chemoresistance in ovarian cancer has been revealed in previous studies.[2,18,21–23] circRNA expression profiles were screened using samples collected from DDP-resistant ovarian cancer patients and DDP-sensitive individuals as controls.[15] The results indicated that 148 circRNAs were upregulated and 191 circRNAs were downregulated, suggesting that circRNAs play a crucial role in regulating chemoresistance in ovarian cancer.[15] In addition, a recent study showed that silencing of hsa_circ_0061140 suppressed ovarian cancer cell proliferation, migration and EMT both in vivo and in vitro through miR-370 sponge activity.[19] In the present study, we showed that circ_C20orf11 is upregulated in the DDP-resistant ovarian cancer cell lines SKOV3/DDP and A2780/DDP. Silencing of circ_C20orf11 in both cell lines suppressed cell proliferation, increased cell apoptosis and, notably, suppressed cell DDP resistance. Increasing evidence suggests that regulatory effects of circRNAs on gene expression occur through competitive binding to miRNAs.[19] We investigated a regulatory mechanism involving miR-527/YWHAZ. miR-527 was previously reported to act as a tumor-suppressive miRNA in many cancer types, such as lung cancer and glioma.[22,24,25] The mechanism by which circ_C20orf11 regulates miR-527 expression was characterized using a luciferase reporter assay. The results showed that circ_C20orf11 directly bound to the 3′-UTR of miR-527. Silencing of circ_C20orf11 in SKOV3/DDP and A2780/DDP cells promoted miR-527 expression. In contrast, downregulation of miR-527 rescued the silencing of circ_C20orf11-induced inhibition of cell viability and proliferation and YWHAZ and IL-10 expression. Additionally, we found that YWHAZ is a direct target of miR-527. YWHAZ has been reported to be involved in regulation of tumorigenesis and drug resistance in ovarian cancer.[26] Consistent with this, our data suggested that circ_C20orf11 regulates YWHAZ expression by acting as a competing endogenous RNA for miR-527 binding and thereby mediates DDP resistance. Finally, in vivo experiments confirmed that knockdown of circ_C20orf11 enhanced DDP sensitivity in vivo. To the best of our knowledge, this is the first study to demonstrate the crucial role of circ_C20orf11 in regulating chemoresistance in ovarian cancer.

Accumulating evidence has demonstrated that EVs are involved in each cancer process, including angiogenesis, drug resistance, and metastasis.[12–14,27–30] Here, we showed that EVs from DDP-resistant ovarian cancer cells can be internalized by M2 macrophages and induce macrophage M2 polarization. Consistently, Liang et al. reported that EVs from colorectal cancer cells transported RPPH1 and promoted macrophage polarization. Many studies have suggested that EVs extracted from tumor cells contain lncRNAs.[13] In this study, we showed that circ_C20orf11 expression was detectable in EVs extracted from the serum of ovarian cancer patients and that circ_C20orf11 was less expressed in the DDP-sensitive group than in the DDP-resistant group. Furthermore, enhanced EV-circ_C20orf11 expression was associated with a poor survival rate of ovarian patients. Based on these data, we suggest that EVs secreted by ovarian cancer cells contain circ_C20orf11 and that circ_C20orf11 may be transferred by EVs to enhance macrophage M2 polarization and regulate tumor macrophages to facilitate DDP resistance. Nevertheless, this regulatory function and the underlying mechanism remain to be further elucidated.

In conclusion, this study provides evidence that circ_C20orf11 enhances DDP resistance in ovarian cancer by inhibiting miR-527/YWHAZ and enhancing EV-mediated macrophage M2 polarization. Thus, EV-circ_C20orf11 may be used as an indicator of DDP sensitivity in ovarian cancer patients.

Materials and methods

Cell culture and treatment

Primary cultured human normal ovarian epithelial cells were cultured in ovarian epithelial cell medium (Gibco, Carlsbad, CA, USA) containing 10% fetal bovine serum (FBS; Gibco) and 1% penicillin (Gibco). THP-1 cells, a human monocytic cell line, were maintained in RPMI-1640 (Invitrogen, Shanghai China) supplemented with 10% FBS and 1% penicillin/streptomycin. THP-1 cells were treated with PMA (phorbol 12-myristate 13-acetate; Sigma-Aldrich, St. Louis, MO) at a concentration of 10 ng/mL in RPMI 1640 supplemented with 1% FBS. The treatment was refreshed every three days until day 6. Human ovarian surface epithelial cells (HOSEpiCs) and the ovarian cancer cell lines SKOV3, A2780, IGROV1, OVCAR-3, and CAOV-3 were maintained in DMEM (Gibco) supplemented with 10% FBS and 1% penicillin. DDP was purchased from Dalian Meilun Biotech Co. (Dalian, China). DDP-resistant A2780/DDP and SKOV3/DDP cells were generated as previously described.[21] In brief, original parental A2780 or SKOV3 cells were exposed to the IC50 concentration of DDP for at least 6 months.

Animal study

Twenty four-week-old male BALB/c-nu mice weighing 21–23 g were purchased from the Shanghai Laboratory Animal Center (SLAC; Shanghai, China) and housed in a controlled environment with a 12-hour light/12-hour dark cycle. This study was approved by the Animal Care and Utilization Committee of Affiliated Tumor Hospital of Xinjiang Medical University and carried out according to the Guidelines for the Care and Use of Laboratory Animals. In this study, mice were separated into four groups (n = 5 per group). Mice were subcutaneously injected with PBS (100 μL) containing approximately 2×10^6 A2780/DDP or SKOV3/DDP cells transfected with si-NC or si-circ_C20orf11 (Genepharma, Shanghai, China). DDP (5 mg/kg, twice a week) was intraperitoneally injected into mice, and the tumor volume was measured every five days. Animals were sacrificed at 30 days following treatment, and tumor tissues were isolated, photographed, and stored in liquid nitrogen for further analyses.

Clinical samples

Sixty paired ovarian cancer tissues and matched adjacent normal tissues were obtained from The Affiliated Tumor Hospital of Xinjiang Medical University and stored in liquid nitrogen until use. For EV purification, the morning fasting venous blood of all subjects (5 mL) was centrifuged, and the serum was preserved at −70°C. Among the 60 patients, 26 were DDP-sensitive, and 34 were DDP-resistant. Patients were considered DDP resistant if they showed no significant clinical effect or had progressive disease after receiving one cycle of DDP treatment. The remaining patients were considered DDP sensitive. The study was approved by the Medical Ethics Committee of The Affiliated Tumor Hospital of Xinjiang Medical University.

MTT assay

MTT assays were used to assess cell viability. In brief, cells were trypsinized and reseeded into 96-well plates (5×10^3/well). Cells were incubated with serial concentrations of DDP (0, 5, 10, 20, 40, or 80 μM) for 24 h. Afterward, MTT solution was added to each well at a final concentration of 0.5 mg/mL (Sigma-Aldrich, St. Louis, USA) and incubated with the cells for 5 h. Absorbance was assessed at 570 nm with a microplate reader (BIO-RAD microplate reader-550). The half-maximal inhibitory concentration (IC50) was measured accordingly.

Cell transfection

Cells were transfected with circ_C20orf11 siRNA, miR-527 mimic, miR-527 inhibitor, or the correlated negative controls obtained from GenePharma for 24 h utilizing Lipofectamine 2000 (Invitrogen). After transfection, the cells were treated with DDP at half of the IC50 dose for 24 h or with DDP at different dilutions accordingly.

Cell colony formation assay

Cell proliferation was assessed using colony formation assays. Briefly, the treated cells were trypsinized, and 200 cells were seeded into each well of a 24-well culture plate containing 2 mL DMEM supplemented with 10% FBS and 1% penicillin. After 7 days of incubation, all the medium was removed. Subsequently, the cells were fixed using 100% methanol (Sigma-Aldrich) for 20 min and stained using crystal violet staining solution (Sigma-Aldrich) for 5 min. Then, the cells were washed with distilled water. The number of colonies was quantified based on brightfield images obtained with a Leica microscope (Leica Microsystems SAS, Wetzlar, Germany).

Cell apoptosis assay

An Annexin-V-FITC/PI apoptosis assay kit (Sigma-Aldrich) was used to stain cells according to the manufacturer's instructions. Flow cytometry (Aceabio, San Diego, USA) was used to analyze the percentage of apoptotic cells.

EV isolation and characterization

EVs were isolated from cells using a total EV isolation reagent based on previously published studies.[11] In detail, cells were incubated with 10% bovine exosome-depleted FBS (Gibco) for 24 h. Subsequently, the medium was collected and centrifuged at 2000 × g for 30 min, after which the supernatant was filtered using a 0.22-mm filter (Sigma-Aldrich). The samples were centrifuged at 10,000 × g at 4°C for 1 h. After the supernatant was removed, the EV pellets were suspended in 150 μL PBS. EVs were measured using an electron microscope or a NanoSight instrument or used for western blot experiments.

EV uptake experiment

PKH67 Fluorescent Cell Linker Mini Kits (Sigma-Aldrich) were used to label the EVs according to the manufacturer's

instructions. Briefly, 1×10^5 THP-1 cells were seeded into 24-well plates. THP-1 cells were cultured with EVs labeled with PKH67 in the dark for 12 h and subsequently fixed with paraformaldehyde and stained with 2,4-diamino-5-phenylthiazole (DAPI; Sigma-Aldrich). Fluorescence images were obtained via laser scanning microscopy.

Dual-luciferase reporter assay

Tt was predicted using the CircInteractome prediction tool, in which circ-C20orf11 was bound to miR-527. The circ_C20orf11 wild-type sequence (C20orf11-WT) containing the miR-527 binding site or a mutant sequence (C20orf11-MUT) were amplified and cloned into a pmirGLO dual-luciferase vector (Promega, Madison, WI, USA). The cells were cotransfected with C20orf11-WT or C20orf11-MUT and miR-527 mimic or miR-527 inhibitor using Lipofectamine 2000 transfection reagent (Invitrogen). A Dual-Luciferase Reporter assay kit (Promega) was used to measure luciferase activities according to the manufacturer's instructions. Similarly, the CircInteractome prediction tool predicted that miR-527 binds to YWHAZ. Therefore, the YWHAZ wild-type sequence (YWHAZ-WT) containing the miR-527 binding site or a mutant sequence (YWHAZ-MUT) were amplified and cloned into a pmirGLO dual-luciferase vector. The cells were cotransfected with YWHAZ-WT or YWHAZ-MUT and miR-527 mimic or miR-527 inhibitor. The Dual-Luciferase Reporter assay kit was used to measure luciferase activities. Luciferase activity was measured using a Promega Luciferase Assay based on the manufacturer's protocol. In brief, 20 μl of each lysate was added to a luminometer tube. Promega Luciferase Assay Substrate was thawed and added to the tube at room temperature.

Enzyme-linked immunosorbent assays (ELISAs)

ELISA kits for IL-10 and IL-6 (Abcam, Cambridge, UK) were utilized according to the manufacturer's instructions. Briefly, 100 μL of cell medium was tested per well. Values were assayed in triplicate and calibrated against IL-10 and IL-6 standards.

Real-time qPCR

Total RNA was extracted from cells or tissues using an RNA extraction kit (Tiangen Biotech, Beijing, China). A Nanodrop spectrophotometer (ND-100; Thermo Scientific, Waltham, MA) was used to detect RNA concentrations based on absorbance at 260/280 nm. Subsequently, the total RNAs were reverse transcribed to complementary cDNA using M-MLV reverse transcriptase (TianGen Biotech). PCR detection was performed with a SYBR Green kit (Solarbio). All experiments were carried out at least three times. Relative gene expression was normalized to GAPDH and U6 expression using the 2 ($^{-\Delta\Delta}$CT) method.

Western blotting assay

Total protein was extracted from cells or tissues using RIPA buffer (Sigma-Aldrich) supplemented with a protease and phosphatase inhibitor cocktail. Total protein was determined with a BCA protein assay kit (Solarbio). Twenty micrograms of protein was separated via SDS-PAGE and transferred onto PVDF membranes (Schleicher & Schuell, Germany), which were blocked with 5% skim milk. Subsequently, the membranes were incubated with primary antibodies at 4°C overnight. The following antibodies were used: anti-63, anti-TSG101, anti-CD9, anti-YWHAZ and anti-PD-L1 (Abcam). The membrane was probed with a horseradish peroxidase-conjugated secondary antibody (Abcam). To develop the immunoreactive bands of target proteins, an enhanced chemiluminescence kit (Thermo Fisher Scientific, Inc., Waltham, MA, USA) was used. Image-Pro Plus 6.0 software was used to quantify bands of interest.

Flow cytometry

Tissue was cut into small pieces and digested by collagenase A (Roche) plus 1*DNase I (Sigma) at 37°C. Following 30 min of incubation, the digested mixture was filtered through a 40 μm nylon mesh. After centrifugation (1,000 rpm for 8 min at 4°C), the isolated cells were stained using a CD206 antibody (cat. no. 18704-1-AP, Proteintech) according to the manufacturer's instructions. After staining, detection of CD206-positive cells was performed using flow cytometry, and the results were calculated based on the percentage of CD206-positive cells.

Statistical analysis

All experiments were performed at least in triplicate. Unpaired two-tailed Student's t-tests were carried out to compare differences between two groups. In the case of multiple comparisons, one-way analysis of variance (ANOVA) followed by Tukey's post hoc test was used. Categorical data were analyzed using a chi-square test. OS was calculated using the Kaplan-Meier method and a log-rank test. Correlations between circ_C20orf11 and miR-527 and between circ_C20orf11 and CD206 expression were analyzed using Spearman's correlation coefficient. GraphPad Prism 5.0 software was utilized for statistical analysis. The data are expressed as the means ± standard deviation. $P < .05$ was considered statistically significant.

Funding

This work was supported by Natural Science Foundation of Xinjiang Autonomous Region (No.2021D01C403)

Disclosure statement

No potential conflict of interest was reported by the author(s).

Availability of data and material

All data generated or analyzed during this study are included in this article. The datasets used and/or analyzed during the current study are available from the corresponding author on reasonable request.

Ethical approval

This study was approved by the Animal Care and Utilization Committee of Affiliated Tumor Hospital of Xinjiang Medical University and carried out according to the Guidelines for the Care and Use of Laboratory Animals. The study was approved by the Medical Ethics Committee of The Affiliated Tumor Hospital of Xinjiang Medical University.

Consent for publication

The informed consent was obtained from study participants.

Authors' contribution

Conception and study design: Jun Yin, Hai-Yan Huang;
Data acquisition: Ying Long;
Data analysis: Yan Ma;
Manuscript drafting: Maerkeya Kamalibaike;
Manuscript revising: Reyanguli Dawuti, Li Li.

Abbreviations

circRNAs: circulating RNAs; DDP: cisplatin; EVs: extracellular vesicles; FBS: foetal bovine serum; HOSEpiCs: human ovarian surface epithelial cells; IC50: half maximal inhibitory concentration; iNOS: inducible nitric oxide synthase; IL-10: interleukin-10; mRNAs: messenger RNAs; miRNAs: microRNAs; ncRNA: non-coding RNA; PD-L1: programmed death-ligand 1; siRNA: small interfering RNA; TNF-α: tumour necrosis factor-alpha; YWHAZ: tyrosine 3-monooxygenase/tryptophan 5-monooxygenase activation protein zeta.

ORCID

Li Li http://orcid.org/0000-0002-7150-2994

References

1. Rauh-Hain JA, Krivak TC, Del Carmen MG, Olawaiye AB. Ovarian cancer screening and early detection in the general population. Rev Obstet Gynecol. 2011;4(1):15–21.
2. Li Z, Niu H, Qin Q, Yang S, Wang Q, Yu C, Wei Z, Jin Z, Wang X, Yang A, others. lncRNA UCA1 mediates resistance to cisplatin by regulating the miR-143/FOSL2-signaling pathway in ovarian cancer. Mol Ther Nucleic Acids. 2019;17:92–101. doi:10.1016/j.omtn.2019.05.007.
3. Liu Y, Feng Y, Liu H, Wu J, Tang Y, Wang Q. Real-time assessment of platinum sensitivity of primary culture from a patient with ovarian cancer with extensive metastasis and the platinum sensitivity enhancing effect by metformin. Oncol Lett. 2018;16(4):4253–4262.
4. Hasan S, Taha R, Omri HE. Current opinions on chemoresistance: an overview. Bioinformation. 2018;14(2):80–85. doi:10.6026/97320630014080.
5. Agarwal R, Kaye SB. Ovarian cancer: strategies for overcoming resistance to chemotherapy. Nat Rev Cancer. 2003;3(7):502–516. doi:10.1038/nrc1123.
6. Yin M, Shen J, Yu S, Fei J, Zhu X, Zhao J, Zhai L, Sadhukhan A, Zhou J. Tumor-associated macrophages (TAMs): a critical activator in ovarian cancer metastasis. Onco Targets Ther. 2019;12:8687–8699. doi:10.2147/OTT.S216355.
7. Colvin EK. Tumor-associated macrophages contribute to tumor progression in ovarian cancer. Front Oncol. 2014;4:137. doi:10.3389/fonc.2014.00137.
8. Larionova I, Cherdyntseva N, Liu T, Patysheva M, Rakina M, Kzhyshkowska J. Interaction of tumor-associated macrophages and cancer chemotherapy. Oncoimmunology. 2019;8(7):1596004. doi:10.1080/2162402X.2019.1596004.
9. Bardi GT, Smith MA, Hood JL. Melanoma exosomes promote mixed M1 and M2 macrophage polarization. Cytokine. 2018;105:63–72. doi:10.1016/j.cyto.2018.02.002.
10. Ham S, Lima LG, Chai EPZ, Muller A, Lobb RJ, Krumeich S, Wen SW, Wiegmans AP, Möller A. Breast cancer-derived exosomes alter macrophage polarization via gp130/STAT3 signaling. Front Immunol. 2018;9:871. doi:10.3389/fimmu.2018.00871.
11. Cheng L, Wang Y, Huang L. Exosomes from M1-polarized macrophages potentiate the cancer vaccine by creating a pro-inflammatory microenvironment in the lymph node. Molecular Therapy. 2017;25(7):1665–1675. doi:10.1016/j.ymthe.2017.02.007.
12. Wang L, Zhao F, Xiao Z, Yao L. Exosomal microRNA-205 is involved in proliferation, migration, invasion, and apoptosis of ovarian cancer cells via regulating VEGFA. Cancer Cell Int. 2019;19(1):281. doi:10.1186/s12935-019-0990-z.
13. Liang Z-X, Liu H-S, Wang F-W, Xiong L, Zhou C, Hu T, He X-W, Wu X-J, Xie D, Wu X-R, others, LncRNA RPPH1 promotes colorectal cancer metastasis by interacting with TUBB3 and by promoting exosomes-mediated macrophage M2 polarization. Cell Death Dis. 2019;10(11):829. doi: 10.1038/s41419-019-2077-0
14. Kanlikilicer P, Bayraktar R, Denizli M, Rashed MH, Ivan C, Aslan B, Mitra R, Karagoz K, Bayraktar E, Zhang X, others. Exosomal miRNA confers chemo resistance via targeting Cav1/p-gp/M2-type macrophage axis in ovarian cancer. EBioMedicine. 2018;38:100–112. doi:10.1016/j.ebiom.2018.11.004.
15. Zhao Z, Ji M, Wang Q, He N, Circular LY. RNA Cdr1as upregulates SCAI to suppress cisplatin resistance in ovarian cancer via miR-1270 suppression. Mol Ther Nucleic Acids. 2019;18:24–33. doi:10.1016/j.omtn.2019.07.012.
16. Gan X, Zhu H, Jiang X, Obiegbusi SC, Yong M, Long X, Hu J. CircMUC16 promotes autophagy of epithelial ovarian cancer via interaction with ATG13 and miR-199a. Mol Cancer. 2020;19(1):45. doi:10.1186/s12943-020-01163-z.
17. Shen M, Li T, Zhang G, Wu P, Chen F, Lou Q, Chen L, Yin X, Zhang T, Wang J. Dynamic expression and functional analysis of circRNA in granulosa cells during follicular development in chicken. BMC Genomics. 2019;20(1):96. doi:10.1186/s12864-019-5462-2.
18. Quan G, Li J. Circular RNAs: biogenesis, expression and their potential roles in reproduction. J Ovarian Res. 2018;11(1):9. doi:10.1186/s13048-018-0381-4.
19. Chen Q, Zhang J, He Y, Wang Y. Hsa_circ_0061140 knockdown reverses FOXM1-mediated cell growth and metastasis in ovarian cancer through miR-370 sponge activity. Mol Ther Nucleic Acids. 2018;13:55–63. doi:10.1016/j.omtn.2018.08.010.
20. Shen J, Zhu X, Fei J, Shi P, Yu S, Zhou J. Advances of exosome in the development of ovarian cancer and its diagnostic and therapeutic prospect. Onco Targets Ther. 2018;11:2831–2841. doi:10.2147/OTT.S159829.
21. Wang DY, Li N, Cui YL. Long noncoding RNA CCAT1 sponges miR-454 to promote chemoresistance of ovarian cancer cells to cisplatin by regulation of surviving. Cancer Res Treat. 2020;52(3):798-814. doi: 10.4143/crt.2019.498.
22. Liu H, Han L, Liu Z, Gao N. Long noncoding RNA MNX1-AS1 contributes to lung cancer progression through the miR-527/BRF2 pathway. J Cell Physiol. 2019;234(8):13843–13850. doi:10.1002/jcp.28064.
23. Klymenko Y, Nephew KP. Nephew KP Epigenetic crosstalk between the tumor microenvironment and ovarian cancer cells: a therapeutic road less traveled. Cancers. 2018;10(9):295. doi:10.3390/cancers10090295.

24. Huo W, Zhu XM, Pan XY, Du M, Sun Z, Li ZM. MicroRNA-527 inhibits TGF-β/SMAD induced epithelial-mesenchymal transition via downregulating SULF2 expression in non-small-cell lung cancer. Math Biosci Eng. 2019;16(5):4607–4621. doi:10.3934/mbe.2019231.
25. Liu J, Hou K, Ji H, Mi S, Yu G, Hu S, Wang J. Overexpression of circular RNA circ-CDC45 facilitates glioma cell progression by sponging miR-516b and miR-527 and predicts an adverse prognosis. J Cell Biochem. 2020;121(1):690–697. doi:10.1002/jcb.29315.
26. Hong L, Chen W, Xing A, Wu D, Wang S. Inhibition of tyrosine 3-monooxygenase/tryptophan 5-monooxygenase activation protein zeta (YWHAZ) overcomes drug resistance and tumorigenicity in ovarian cancer. Cell Physiol Biochem. 2018;49(1):53–64. doi:10.1159/000492839.
27. Mashouri L, Yousefi H, Aref AR, Ahadi AM, Molaei F, Alahari SK. Exosomes: composition, biogenesis, and mechanisms in cancer metastasis and drug resistance. Mol Cancer. 2019;18(1):75. doi:10.1186/s12943-019-0991-5.
28. Azmi AS, Bao B, Sarkar FH. Exosomes in cancer development, metastasis, and drug resistance: a comprehensive review. Cancer Metastasis Rev. 2013;32(3–4):623–642. doi:10.1007/s10555-013-9441-9.
29. Zhang C, Ji Q, Yang Y, Li Q, Wang Z. Exosome: function and role in cancer metastasis and drug resistance. Technol Cancer Res Treat. 2018;17:1533033818763450. doi:10.1177/1533033818763450.
30. Wu M, Wang G, Hu W, Yao Y, Yu X-F. Emerging roles and therapeutic value of exosomes in cancer metastasis. Mol Cancer. 2019;18(1):53. doi:10.1186/s12943-019-0964-8.